Progress In Electromagnetics Research, PIER 28, 97–120, 2000

DIFFERENTIAL RAIN ATTENUATION STATISTICS INCLUDING AN ACCURATE ESTIMATION OF THE EFFECTIVE SLANT PATH LENGTHS

J. D. Kanellopoulos, A. D. Panagopoulos, and S. N. Livieratos

Division of Electroscience
Department of Electrical Engineering and Computer Engineering
National Technical University of Athens
9 Iroon Polytechniou Street
Zografou, GR-15773
Athens, Greece

1. INTRODUCTION

One serious problem of interference between adjacent satellite paths operating at the same frequency and separated by a small angle θ as viewed from an Earth station (Fig. 1) is considered to be the differential rain attenuation. Because of the spatial inhomogeneity in the precipitation medium, periods of time can exist in which the signal may suffer a large attenuation A_C in comparison with the attenua-

tion A_I of the unwanted signal. When this difference $\Delta A = A_C - A_I$ becomes sufficiently large, the unwanted signal from the adjacent satellite path can cause interference. In order to calculate the amount of induced interference, the distribution of the differential rain attenuation ΔA should be used, under the condition of proper operation, i.e., when the rain attenuation has not yet exceeded the system power margin M (dB) but is always greater than a minimum measurable attenuation threshold r_m ($r_m < A_C < M$). In this sense, Rogers et al. [1] have first proposed an empirical model for the prediction of the differential rain attenuation ΔA at the 1% conditional probability level. As suggested by CCIR [2], the above model although simple is provisional and must be used with caution. For this reason, Kanellopoulos et al. [3] have proposed a more general predictive method for the evaluation of the differential rain attenuation statistics based on a model of convective raincells and the lognormal assumption for the point rainfall statistics. In the above analysis, a simplified constant rain height equal to the height of the 0°C isotherm, dependent upon the latitude of the location [4], has been used. Further, Kanellopoulos and Margetis [5] have most recently modified the latter predictive method by considering a more realistic model for the effective rain height, consisting of using the 0°C isotherm height for low rainrates and adding a rainrate dependent term for higher rainrates. The adoption of the above rain height model has been shown there [5] that is quite successful and generally improves the comparison between theoretical results and available simulated interference data [1]. On the other hand, the latter consideration is based on an assumption for the calculation of the effective slant paths which is rather suitable for satellite paths operating under relative high elevation angles (greater than about 30°–40°). For this reason, a more accurate estimation of the effective slant path lengths in the general case is needed and this is the subject of the present paper. Numerical results taken from the modified procedure are compared with the available set of simulated data in Montreal area. In addition, the influence of various other parameters such as the geographic latitude and climatic zone is also investigated.

2. THE ANALYSIS

The detailed configuration of the problem is shown in Fig. 1. The two satellite paths have different elevation angles φ_1, φ_2 and they are separated from one another by a small angle θ_d as viewed from Earth

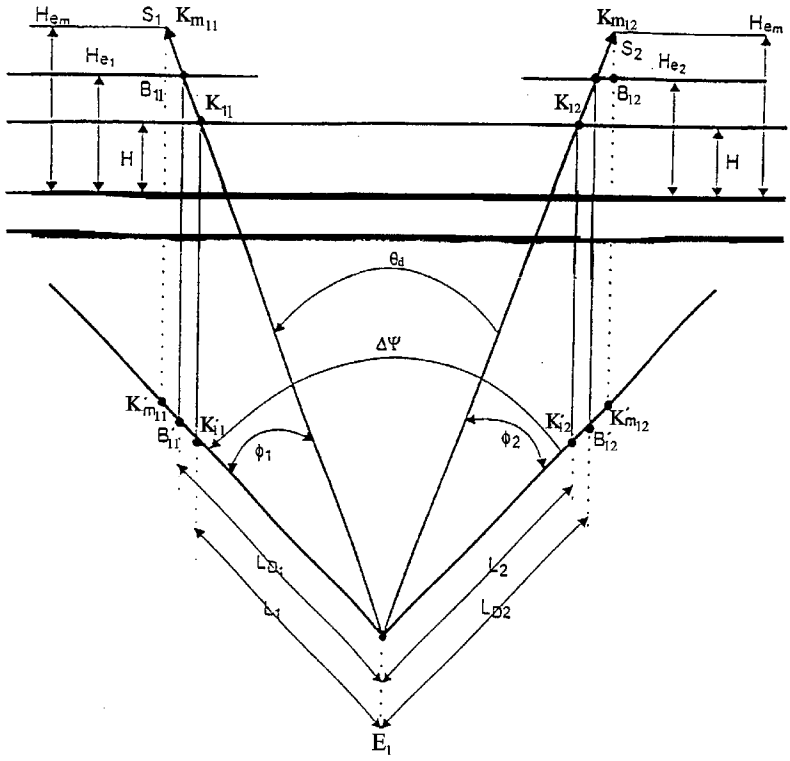

Figure 1. Configuration of the system.

station. $\Delta\psi$ is also the projected differential angle between the slant paths under consideration. The other parameters encountered in Fig. 1 will be described in Subsection 2.1. As it happens with problems of this kind, the main point of the interference analysis is the evaluation of the differential attenuation statistics given by:

$$P[\Delta A \geq r | r_m \leq A_C \leq M] = \frac{P[\Delta A \geq r, r_m \leq A_C \leq M]}{P[r_m \leq A_C \leq M]} \qquad (1)$$

where r is the exceeded differential attenuation level and the minimum measurable attenuation threshold r_m is usually taken to be $0.5\,\mathrm{dB}$, as Rogers et al. [1] have suggested.

2.1 General Considerations

The following considerations are taken into account :
(a) Crane's simplified considerations for the vertical variation of the rainfall structure are first employed [4]. This leads to the assumption of uniform rain structure from the ground up to an effective rain height H_e. For the determination of the rain height H_e, we consider here the model proposed by Stutzman and Dishman [6], as has also been used by Kanellopoulos an Margetis [5] for the same reason. According to this consideration, we have:

$$H_e = \begin{cases} H & \text{for } R \leq 10\,\text{mm/hr} \\ H + \log\left(\dfrac{R}{10}\right) & \text{for } R \leq 10\,\text{mm/hr} \end{cases} \tag{2}$$

where

$$H = \begin{cases} 4.8\,\text{Km} & |\Lambda| \leq 30^\circ \\ \left(7.8 - 0.1\dfrac{|\Lambda|}{\text{deg}}\right)\,\text{Km} & |\Lambda| > 30^\circ \end{cases} \tag{3}$$

where Λ is the latitude of the location of the Earth terminal and R is the value of the rainfall rate at the specific point. It should be noted here that the above formulas concern mean seasonal values for H_e and H as it is proper for long-term rain attenuation statistics. For the proceeding analysis the definition of some characteristic points is needed. These are the section points K_1, K_2 and K_{m_1}, K_{m_2} between the slant paths ES_1, ES_2 and the levels H and H_{em} respectively. The effective rain height H_{em} is evaluated by means of Eq. (2) and is related to some maximum observed rainfall rate (say 150–200 mm/hr). One of the complications of the analysis is the fact that the rain height H_e varies generally with rainrate (see also expression (2)). As a direct result the effective slant path length is also a function of the rainfall rate values referring to all points inside the part $K_i'K_{m_i}'$ (see Fig. 1), for rainrates greater than 10 mm/hr. In order to avoid the above consideration, which leads to cumbersome and very complicated calculations, the homogeneity of the rainfall medium inside the part $K_i'K_{m_i}'$ has been assumed by Kanellopoulos and Margetis [5]. However, this assumption can be shown to be quite reasonable for elevation angles greater than about 30°, leading to projected straightline parts of the order of few kilometers. For satellite paths operating under elevation angles not satisfying the above condition, the induced error in our calculations, due to non accurate estimation of the effective slant path

length, becomes appreciable and thus this assumption should be properly revised. For this reason, the rainfall inhomogeneity inside the part $K_i'K_{m_i}'$ should be taken into account, and one of the appropriate ways is to adopt the following simulated spatial profile, as suggested by Stutzman and Dishman [6]

$$R(z) = \begin{cases} R & \text{for } R \leq 10\,\text{mm/hr} \\ R \cdot \exp\left[-\gamma \ln\left(\dfrac{R}{10}\right) z\right] & \text{for } R > 10\,\text{mm/hr} \end{cases} \tag{4}$$

where $\gamma = 1/22$ and the rainfall rate refers to the point K_1' or K_2'. As pointed out by the same authors [6], the adoption of the above simulated spatial profile does not contradict with the notion of raincells, which can be assumed for the description of the rainfall inhomogeneity inside the effective slant path lengths EK_1' and EK_2' (see Fig. 1). Further, it can be shown that introduction of the above simulated spatial profile is equivalent to the consideration that the rainfall medium inside the parts $K_1'K_{m_1}'$, $K_2'K_{m_2}'$ behaves like an homogeneous one with equivalent rainfall rate $(R_{\text{ave}})_i$ given by:

$$(R_{\text{ave}})_i = \frac{1}{D_i} \int_0^{D_i} R(z)dz \tag{5}$$

that is :

$$(R_{\text{ave}})_i = \begin{cases} R_{K_i} & \text{for } R_{K_i} \leq 10\,\text{mm/hr} \\ R_{K_i} \dfrac{1 - \exp\left[-\gamma \ln\left(\dfrac{R_{K_i}}{10}\right) D_i\right]}{\gamma \ln\left(\dfrac{R_{K_i}}{10}\right) D_i} = c_i R_{K_i}^{d_i} & \\ & (i = 1, 2) \quad \text{for } \mathrm{R_{K_i}} > 10\,\text{mm/hr} \end{cases} \tag{6}$$

and

$$D_i = \frac{\log\left(\dfrac{R_{K_i}}{10}\right)}{\tan \varphi_i} \quad (i = 1, 2) \tag{7}$$

In the above expressions, c_i and d_i are constants depending on the elevation angle φ_i and they are derived by means of an appropriate regression fitting procedure.

Following this assumption the effective slant paths are now given by:

$$L_{s_i} = \frac{H_{e_i} - H_o}{\sin \varphi_i} \quad (i = 1, 2) \tag{8}$$

where the levels H_{e_i} $(i = 1, 2)$ depend upon the rainfall rates $(R_{\text{ave}})_i$ with respect to K_i (see expressions (5–7)), in accordance with expression (2), with R substituted by $(R_{\text{ave}})_i$ there. Moreover, H_o is the average height of the Earth station above sea level.
(b) All the other assumptions concerning the point rainrate statistics, the specific rain attenuation $(A_o = aR^b)$ and the horizontal structure of the rainfall medium are the same as those employed for the analysis of the previous methodology [3, 5]. For the latter consideration, we assume that the convective raincells model proposed by Lin [7] is taken to be valid with respect to effective slant path lengths EK_1' and EK_2'.

2.2 Evaluation of the Differential Attenuation Probability

Following the previous considerations, the single and joint exceedance probabilities encountered in equation (1) can be expressed analytically in terms of the statistical parameters A_{m_1}, S_{α_1} and A_{m_2}, S_{α_2} concerning the attenuations A_C' and A_I', as well as the logarithmic correlation coefficient ρ_{n12} between them. A_C' and A_I' are the attenuations referring to hypothetical terrestrial links being the projections of the slant paths ES_1 and ES_2 affected by the rain.

It should be emphasized here that the novel considerations examined here influence only the calculation of the parameters A_{m_1}, S_{α_1}, A_{m_2}, S_{α_2} and $\rho_{n_{12}}$ and not the forms of the above exceedance probabilities. However, in order to have a complete view of the whole problem, these expressions are briefly presented in Appendix A.

Further the parameters A_{m_1}, S_{α_1} and A_{m_2}, S_{α_2} are expressed as [8]:

$$\left.\begin{aligned} S_{\alpha_i}^2 &= \ln\left[\frac{\sigma_{A_i}^2}{\mu_{A_i}^2} + 1\right] \\ A_{m_i} &= \frac{\mu_{A_i}^2}{\sqrt{\sigma_{A_i}^2 + \mu_{A_i}^2}} \end{aligned}\right\} \quad (i = 1, 2) \tag{9}$$

in terms of the mean values (μ_{A_i}) and standard deviations (σ_{A_i}) of the variables A_C' and A_I', respectively. Following now a straightforward analysis, the μ_{A_i} and σ_{A_i} can be calculated by means of the

R_m (median value) and S_r (standard deviation) concerning the point rainfall distribution, the constants a and b of the specific rain attenuation ($A_o = aR^b$), and the characteristic distance G appropriate to describe the spatial rainfall inhomogeneity, as suggested by Lin [7]. The final results are presented here, while analytical details for their derivation can be found in Appendix B.

$$\mu_{A_i} = am_b L_i + \frac{am'_{b_i}}{2\tan\varphi_i}\left\{c_i^b \log\left(\frac{c_i}{10}\right)\operatorname{erfc}(t_{o_i}) + c_i^b d_i \log e[\ln(R_m) + bd_i S_r^2]\operatorname{erfc}(t_{o_i}) + \sqrt{\frac{2}{\pi}}c_i^b d_i \log e S_r e^{-t_{o_i}^2}\right\} \qquad (i = 1, 2) \quad (10)$$

where

$$L_i = \frac{H - H_o}{\tan\varphi_i} \quad (11)$$

$$m_b = R_m^b \exp\left(\frac{b^2 S_r^2}{2}\right) \quad (12)$$

$$m'_{b_i} = R_m^{bd_i} \exp\left(\frac{b^2 d_i^2 S_r^2}{2}\right) \quad (13)$$

$$t_{o_i} = \frac{u_o - bd_i S_r}{\sqrt{2}} \quad (14)$$

$$u_o = \frac{\ln(10/R_m)}{S_r} \quad (15)$$

and

$$\left.\begin{aligned}\sigma_{A_1}^2 &= E[A_C'^2] - \mu_{A_1}^2 \\ \sigma_{A_2}^2 &= E[A_I'^2] - \mu_{A_2}^2\end{aligned}\right\} \quad (16)$$

where

$$\left.\begin{aligned}E[A_C'^2] &= M_{11} + 2M_{1d} + M_{dd1} \\ E[A_I'^2] &= M_{22} + 2M_{2d} + M_{dd2}\end{aligned}\right\} \quad (17)$$

Further we have :

$$M_{ii} = a^2\sigma_b^2 H_{ii} + a^2 m_b^2 L_i^2 \quad (18)$$

$$\sigma_b^2 = m_{2b} - m_b^2 \quad (19)$$

$$m_{2b} = R_m^{2b} \exp(2b^2 S_r^2) \quad (20)$$

$$H_{ii} = 2L_i G \sin h^{-1}\left(\frac{L_i}{G}\right) + 2G^2\left[1 - \left[\left(\frac{L_i}{G}\right)^2 + 1\right]^{1/2}\right] \quad (i = 1, 2) \tag{21}$$

The analytical expressions for M_{1d}, M_{2d} and M_{dd1}, M_{dd2} can be found in Appendix B.

In addition the calculation of ρ_{n12} which is the logarithmic correlation coefficient between A'_C and A'_I follows quite similar steps. More particularly, we have [3]:

$$\rho_{n12} = \frac{1}{S_{\alpha_1} \cdot S_{\alpha_2}} \ln\left[1 + \rho_{12}\sqrt{(e^{S^2_{\alpha_1}} - 1)(e^{S^2_{\alpha_2}} - 1)}\right] \tag{22}$$

and the path correlation coefficient ρ_{12} is expressed as :

$$\rho_{12} = \frac{E\{A'_C A'_I\} - \mu_{A_1} \cdot \mu_{A_2}}{\sigma_{A_1} \cdot \sigma_{A_2}} \tag{23}$$

Following again a similar statistical analysis, as before for the μ_{A_i} and σ_{A_i} , one gets:

$$E[A'_C \cdot A'_I] = N_{12} + N_{1d} + N_{2d} + N_{dd} \tag{24}$$

where

$$N_{12} = a^2\sigma_b^2 H_2 + a^2 m_b^2 L_1 L_2 \tag{25}$$

and the analytical expressions for H_2 can be found elsewhere [3], where the constant 0° isotherm for the rain height has been considered (see expression (3)). The other terms of (24) are complicated but analytical expressions of R_m, S_r; a, b, G, c_i, d_i, φ_i and are presented in Appendix C, where details for their derivation are also included.

3. NUMERICAL RESULTS AND DISCUSSION

In this section, an application of the above analysis is presented. The numerical results are first compared with available simulated data in the open literature taken from Rogers et al. [1] in the Montreal area. Details concerning the derivation of the above data and other useful information can be found elsewhere [1, 5]. Further, the implementation

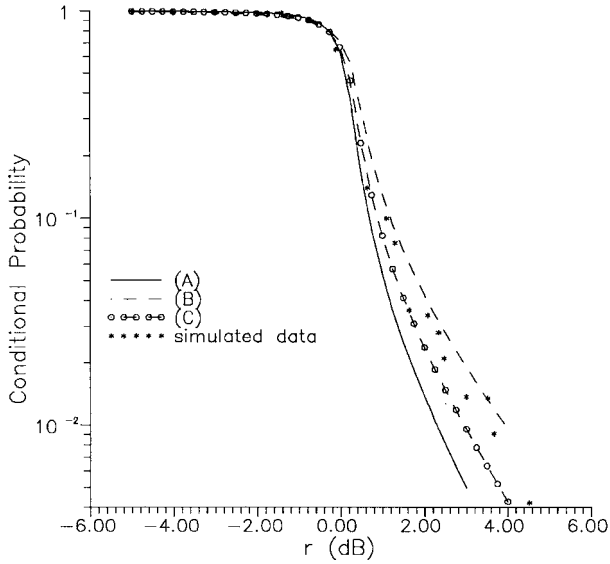

Figure 2. The conditional probability $P[\Delta A \geq r | r_m \leq A_C \leq M]$ versus the variable r for $f = 15\,\mathrm{GHz}$, $M = 10\,\mathrm{dB}$, $\varphi_1 = \varphi_2 = 10^\circ$, $\theta_d = 6^\circ$ (Montreal area).
(A): MODEL USING CONSTANT RAIN HEIGHT
(B): KANELLOPOULOS AND MARGETIS MODEL
(C): PRESENT MODEL

of the proposed procedure requires the knowledge of the parameters H, H_o, a, b, G, R_m and S_r with respect to the Montreal data under consideration. A list of appropriate numerical values for these parameters can also be found elsewhere [5]. In Figure 2, the conditional probability has been drawn versus the variable r (in dB) in comparison with the simulated data. An interfered satellite path operating at $f = 15\,\mathrm{GHz}$ with an elevation angle $\varphi_1 = 10^\circ$ has been considered. The interfering path has also $\varphi_2 = 10^\circ$. In the same figure, the results taken from the existing predictive procedures [3, 5] are also drawn. As can be seen, the comparison shows a tendency of better approximation in relation to the already existing predictive results. In addition, the differential attenuation at the 1% conditional probability $\Delta A(1\%)$ is further examined. More particularly, in Fig. 3, (available margin in decibels) curve versus the angular separation θ_d (in degrees) is shown for $\Delta A(1\%) = 3\,\mathrm{dB}$, $f = 15\,\mathrm{Hz}$, $\phi_1 = \phi_2 = 10$. A more improved situation with respect to the experimental data is obvious here. Gen-

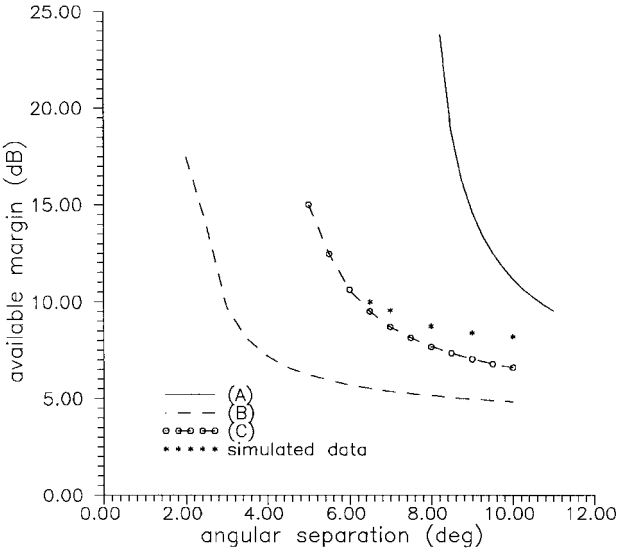

Figure 3. Available margin M (in dB) versus the angular separation θ_d (in degrees) for $f = 15\,\text{Hz}$, $\phi_1 = \phi_2 = 10°$, $\Delta A(1\%) = 3\,\text{dB}$ (Montreal area).
(A): MODEL USING CONSTANT RAIN HEIGHT
(B): KANELLOPOULOS AND MARGETIS MODEL
(C): PRESENT MODEL

erally, the results of the present model fall between the constant rain height and the Kanellopoulos and Margetis models. In order to be more specific, we present here the error estimates of the new results in comparison with the other predictive models. As a matter of fact, for each level of available margin M the percentage error e corresponding to the calculated value of the angular separation is given by

$$e = \frac{\theta_{d,p} - \theta_{d,m}}{\theta_{d,m}} \times 100\% \tag{26}$$

where $\theta_{d,p}$ is the predicted (in deg) and $\theta_{d,m}$ the measured angular separation (in deg). The above error value has been estimated for all the experiments where M versus θ_d data are available [1]. Further, the mean μ_e, standard deviation σ_e and $r.m.s$ value ($r.m.s = \sqrt{\mu_e^2 + \sigma_e^2}$) of the error estimates have been evaluated and presented in Table 1 for various levels of margin M (in dB). As it is obvious,

the present model produces the smallest μ_e, σ_e and $r.m.s$ value. As a first conclusion, the necessity for the development of the present method, using more accurate estimations for the effective slant path lengths, seems to be justified.

Table 1. Error estimates for various levels of margin M.

Present Model

Margin threshold (M)	3 dB	4 dB	5 dB	6 dB	7 dB	8 dB	9 dB	10 dB	11 dB	12 dB
μ_e	−2.05	−5.05	−3.63	−5.53	−3.43	−5.69	−0.69	−2.72	−1.11	2.91
σ_e	4.86	6.30	4.57	5.56	4.49	15.04	0.67	0.21	0.25	0.32
D_e	5.27	8.07	5.84	7.84	5.65	16.08	0.96	2.73	1.14	2.93

Kanellopoulos and Margetis Model

Margin threshold (M)	3 dB	4 dB	5 dB	6 dB	7 dB	8 dB	9 dB	10 dB	11 dB	12 dB
μ_e	−31.91	−37.355	−35.88	−32.68	−25.82	−26.52	−37.65	−37.31	−22.25	23.51
σ_e	10.24	13.24	10.23	10.01	11.69	19.62	16.55	15.75	14.37	16.82
D_e	33.51	39.63	37.31	34.18	28.34	32.99	41.13	40.49	26.49	28.91

Constant Rain Height Model

Margin threshold (M)	3 dB	4 dB	5 dB	6 dB	7 dB	8 dB	9 dB	10 dB	11 dB	12 dB
μ_e	48.77	43.75	54.08	56.28	60.12	71.91	67.91	71.12	80.61	85.92
σ_e	12.14	17.75	13.64	15.79	24.98	38.09	11.70	10.47	22.46	21.41
D_e	50.26	47.21	55.77	58.45	65.11	81.38	68.91	71.89	83.68	88.55

In the following part of the section, similar curves as before are examined for some other locations where experimental data are not available. More particularly in Figures 4–5, the conditional probability versus r is drawn for a location in Denmark. For the examined case, we have considered $f = 12\,\mathrm{GHz}$, $\theta_d = 3^\circ$, $M = 10\,\mathrm{dB}$ and elevation angles ranging from 10° to 30°. As it can be seen, the deviation between the present results and the existing ones [3, 5] is rather insignificant for satellite paths corresponding to $\varphi = 30^\circ$ elevation angles (Fig. 4). On the other hand, there is a gradually increasing deviation with the decrease of the elevation angle and this is quite pronounced for $\varphi = 10^\circ$ (Fig. 5). This is an expectable fact in absolute agreement with the fundamental assumption of the present paper.

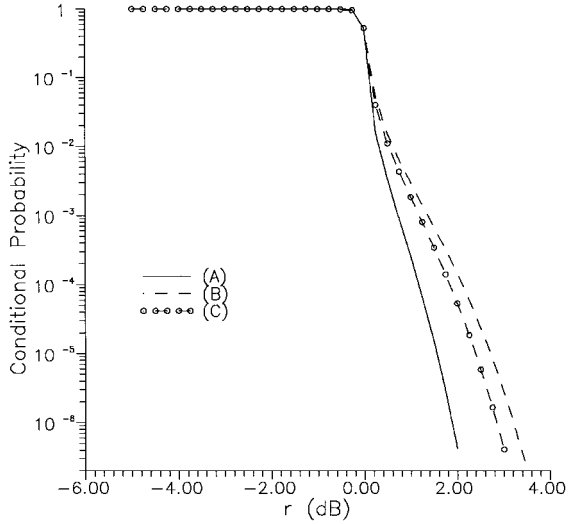

Figure 4. The conditional probability $P[\Delta A \geq r | r_m \leq A_C \leq M]$ versus the variable r for $f = 12\,\mathrm{GHz}$, $M = 10\,\mathrm{dB}$, $\varphi_1 = \varphi_2 = 30^\circ$, $\theta_d = 3^\circ$ (Denmark area).
(A): MODEL USING CONSTANT RAIN HEIGHT
(B): KANELLOPOULOS AND MARGETIS MODEL
(C): PRESENT MODEL

Another set of curves very useful for the system designer concerns the examination of the effective carrier to interference ratio (C/I) versus the angular separation θ_d of the two satellites. Following basic link considerations [9], the (C/I) ratio of an Earth-space system interfered by an adjacent satellite under clear sky conditions can be expressed as

$$\left(\frac{C}{I}\right)_{\text{c.s.}} = P + Q \cdot \log \theta_d \tag{27}$$

where the constants P and Q depend upon the equivalent isotropic radiated power of interfered satellite $S_1\, EIRP_s$, the equivalent isotropic radiated power of interfering satellite $S_2\, EIRP'_s$ and the characteristics of the sidelobe envelope level of the received antenna [9]. Under rain fade conditions the $(\frac{C}{I})$ ratio is reduced in the following way,

$$\left(\frac{C}{I}\right) = \left(\frac{C}{I}\right)_{\text{c.s.}} - \Delta A \tag{28}$$

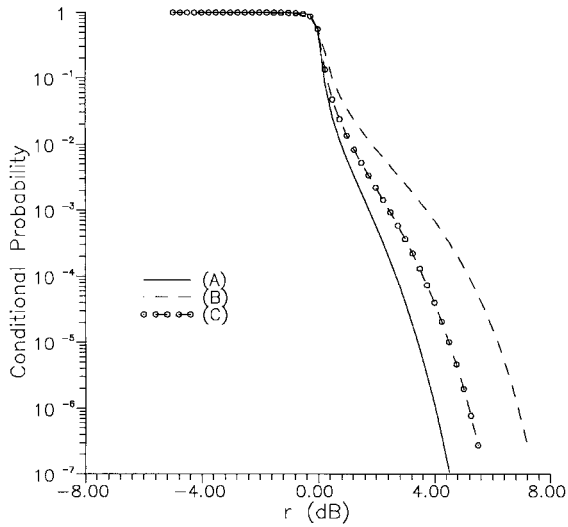

Figure 5. The same as in Fig. 4 but for $\varphi_1 = \varphi_2 = 10^\circ$.

In Figures 6–7, curves of (C/I) versus θ_d are presented for an Earth station located in Denmark with respect to two elevation angles (10° and 30°). The numerical values for P and Q (see expression (27)) are presented in Table 2. For both cases, the frequency has been taken to be 12 GHz, whereas an outage time of the order of 30 minutes has been considered. Moreover, the percentage conditional interference probability level in relation to the probability of proper operation, as defined previously, has been assumed to be 0.001% (Fig. 6) and 0.01% (Fig. 7). In the same Figures the predictive results taken from the existing methods [3, 5] are also presented.

Table 2. Parameters of the (C/I) versus θ example.

Parameter	Value
P	15
Q	25

As it is expected, the deviation of the modified results against the existing ones is quite insignificant for the $\varphi = 30^\circ$ elevation angle case. The opposite certainly occurs for $\varphi = 10^\circ$ and this deviation can be very critical, as will be shown in the following example. Let us assume,

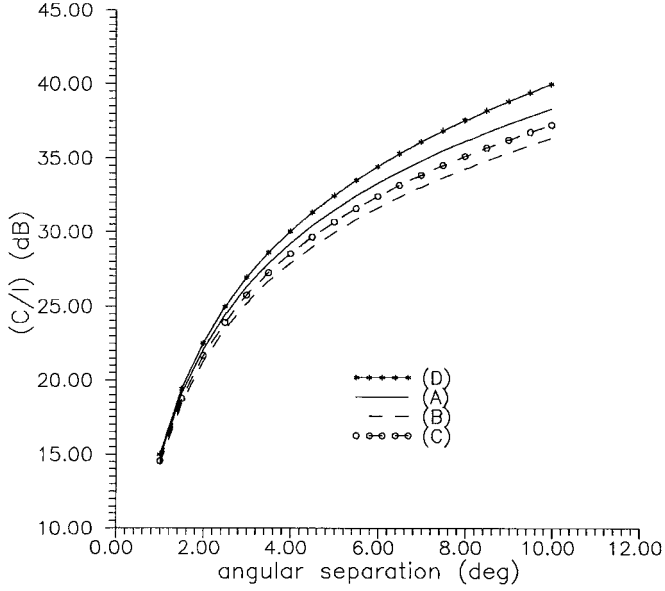

Figure 6. Carrier-to-interference ratio (C/I) versus the angular separation (θ_d) in comparison with the existing predictive results: $f = 12\,\text{GHz}$, $\varphi_1 = \varphi_2 = 30°$, outage time: $30\,\text{min/year}$ and percentage conditional probability: 0.001%, (Denmark area).
(A): MODEL USING CONSTANT RAIN HEIGHT
(B): KANELLOPOULOS AND MARGETIS MODEL
(C): PRESENT MODEL
(D): CLEAR SKY CURVE

that we would like to estimate a threshold θth of the angular separation between the satellites, less than this the operating system violates the specified interference tolerance conditions. By this term, we mean that the $(\frac{C}{I})$ ratio is permitted to exceed an established "power protection ratio" for cochannel interference with respect to a specified conditional probability $p\%$. If we would specify a "power protection ratio" of the order of $30\,\text{dB}$, valid for both 0.001% and 0.01%, then from Fig. 6 the corresponding θth can be found to be 4 (deg) for the unperturbed model [3], and 5.5 (deg), 6 (deg) for the present and the Kanellopoulos-Margetis models [5], respectively. As can be seen, the influence of the present assumption for the more accurate estimation of the effective slant radio paths is not quite significant in relation to

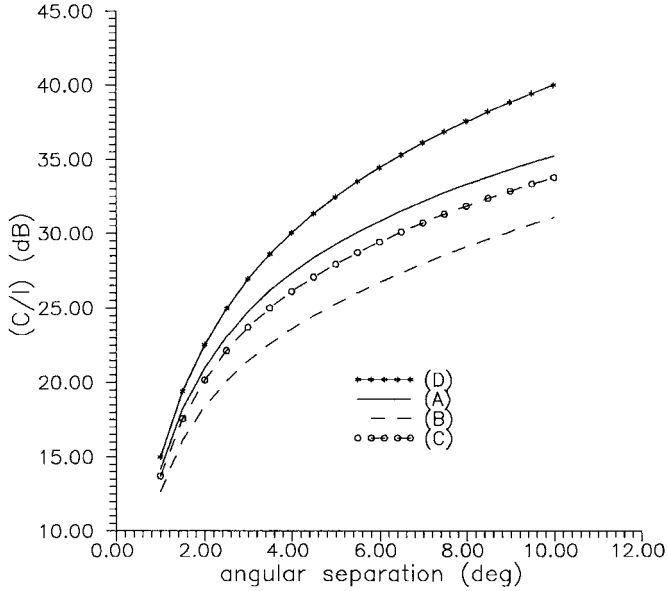

Figure 7. Carrier-to-interference ratio (C/I) versus the angular separation (θ_d) in comparison with the existing predictive results: $f = 12\,\mathrm{GHz}$, $\varphi_1 = \varphi_2 = 10^\circ$, outage time: 30 min/year and percentage conditional probability: 0.01%, (Denmark area).
(A): MODEL USING CONSTANT RAIN HEIGHT
(B): KANELLOPOULOS AND MARGETIS MODEL
(C): PRESENT MODEL
(D): CLEAR SKY CURVE

the Kanellopoulos-Margetis model. This is quite expectable due to the fact that the elevation angle is 30°. On the other hand, for the corresponding $\varphi = 10^\circ$ case (Fig. 7) the respective values are 5, 7 and 10 (deg) and the necessity for introducing the novel assumptions for the more accurate estimation of the effective slant radio path lengths becomes inevitable.

4. CONCLUSIONS

One of the main propagation effects on interference between Earth-space paths is considered to be the differential rain attenuation. In this paper, an existing procedure for the prediction of the differential rain attenuation is properly modified to include a more complicated

but accurate estimation of the effective slant path lengths. This modification is considered to be necessary, particularly for satellite paths operating under low elevation angles in the Ku-Band. The results of the present procedure are compared with simulated data taken from Montreal. The comparison shows an improved situation in relation to the existing methods. In addition, the difference between the existing results and the deduced ones after use of the novel considerations for some other locations and climatic zones is also examined. As a general conclusion, independent of the latitude of the location and the climatic zone, the induced modification is quite significant for interfered satellite paths associated with low elevation angles. On the other hand, for elevation angles greater than about 30°, the improvement is considered to be negligible and the already existing predictive methods may be used.

APPENDIX A. CALCULATION OF THE CONDITIONAL PROBABILITY IN (1)

$$P[r_m \le A_C \le M] = \frac{1}{2}\left(\operatorname{erfc}\left(\frac{u_{00}}{\sqrt{2}}\right) - \operatorname{erfc}\left(\frac{u_{02}}{\sqrt{2}}\right)\right) \tag{A.1}$$

$$P[\Delta A \ge r, r_m \le A_C \le M] = \frac{1}{2}\left[\operatorname{erfc}\left(\frac{u_{01}}{\sqrt{2}}\right) - \operatorname{erfc}\left(\frac{u_{02}}{\sqrt{2}}\right)\right] - \frac{1}{2}\int_{u_{01}}^{u_{02}} f_{U_1}(u_1)\operatorname{erfc}\left[\frac{u_{03} - \rho_{n_{12}}u_1}{\sqrt{2(1-\rho_{n_{12}}^2)}}\right] \quad \text{for} \quad r_m \le r \le M \tag{A.2}$$

$$P[\Delta A \ge r, r_m \le A_C \le M] = \frac{1}{2}\left[\operatorname{erfc}\left(\frac{u_{00}}{\sqrt{2}}\right) - \operatorname{erfc}\left(\frac{u_{02}}{\sqrt{2}}\right)\right] - \frac{1}{2}\int_{u_{00}}^{u_{02}} f_{U_1}(u_1)\operatorname{erfc}\left[\frac{u_{03} - \rho_{n_{12}}u_1}{\sqrt{2(1-\rho_{n_{12}}^2)}}\right] \quad \text{for} \quad r < r_m \tag{A.3}$$

$$P[\Delta A \ge r, r_m \le A_C \le M] = 0 \qquad \text{for} \quad r > M \tag{A.4}$$

In the above expressions we have :

$$u_{00} = \frac{\ln(r_m \cos\varphi_1) - \ln(A_{m_1})}{S_{\alpha_1}} \tag{A.5}$$

$$u_{01} = \frac{\ln(r\cos\varphi_1) - \ln(A_{m_1})}{S_{\alpha_1}} \tag{A.6}$$

$$u_{02} = \frac{\ln(M\cos\varphi_1) - \ln(A_{m_1})}{S_{\alpha_1}} \tag{A.7}$$

$$f_{U_1}(u_1) = \frac{1}{\sqrt{2\pi}}\exp\left(-\frac{u_1^2}{2}\right) \tag{A.8}$$

$$u_{03} = \frac{\ln\left[\exp[u_1 S_{\alpha_1} + \ln A_{m_1}]\dfrac{\cos\varphi_2}{\cos\varphi_1} - r\cos\varphi_2\right] - \ell n A_{m_2}}{S_{\alpha_2}} \tag{A.9}$$

APPENDIX B. EVALUATION OF THE PARAMETERS μ_{A_1}, μ_{A_2}, σ_{A_1}, and σ_{A_2}

According to their definition we have :

$$\begin{aligned}\mu_{A_i} &= E\left\{\int_0^{L_{D_i}} A_o dl\right\} = E\left\{\int_0^{L_i} A_o dl\right\} + E\left\{\int_{L_i}^{L_{D_i}} A_o dl\right\} \\ &= a m_b L_i + E\left\{\int_{L_i}^{L_{D_i}} A_o dl\right\}\end{aligned} \tag{B.1}$$

where L_i are given by (11) and

$$L_{D_i} = L_{S_i}\cos\varphi_i \tag{B.2}$$

Assuming now the inhomogeneity of the rainfall medium inside the part $K_i' K_{m_i}'$ and taking into account the comments preceding expression (7), we have:

$$\begin{aligned}E\left\{\int_{L_i}^{L_{D_i}} A_o dl\right\} &= \frac{a}{\tan\varphi_i} E\left\{(R_{\text{ave}})_i^b \log\left(\frac{(R_{\text{ave}})_i}{10}\right)\right\} \\ &= \frac{a c_i^b}{\tan\varphi_i}\int_{10}^{\infty} r^{bd_i}\log\left(\frac{c_i r^{d_i}}{10}\right) p(r) dr \\ &= \frac{a c_i^b R_m^{bd_i}}{\tan\varphi_i}\int_{u_o}^{\infty} e^{bd_i u S_r}\left[\log\left(\frac{c_i R_m^{d_i} e^{d_i u S_r}}{10}\right)\right] f(u) du\end{aligned} \tag{B.3}$$

where $f(u)$ is the normal density function [8] and u_o is given by (15). After a straightforward algebra, one gets expression (10) of the main

text. Further, following the definitions (16) for the σ_{A_1} , σ_{A_2} , we need to calculate the $E\{A_C'^2\}$ and $E\{A_I'^2\}$ given by:

$$\begin{aligned}
E\{A_C'^2\} &= E\left\{\int_0^{L_{D_1}} dz \int_0^{L_{D_1}} dz' [A_o(z)A_o(z')]\right\} \\
&= \int_0^{L_1} dz \int_0^{L_1} dz' E\{A_o(z)A_o(z')\} \\
&\quad + 2E\left\{\int_0^{L_1} dz \int_{L1}^{L_{D_1}} dz' A_o(z)A_o(z')\right\} \\
&\quad + E\left\{\int_{L_1}^{L_{D_1}} dz \int_{L_1}^{L_{D_1}} dz' A_o(z)A_o(z')\right\} \\
&= M_{11} + 2M_{1d} + M_{dd1} \qquad \text{(B.4)} \\
E\{A_I'^2\} &= E\left\{\int_0^{L_{D_2}} dz \int_0^{L_{D_2}} dz' [A_o(z)A_o(z')]\right\} \\
&= \int_0^{L_2} dz \int_0^{L_2} dz' E\{A_o(z)A_o(z')\} \\
&\quad + 2E\left\{\int_0^{L_2} dz \int_{L2}^{L_{D_2}} dz' A_o(z)A_o(z')\right\} \\
&\quad + E\left\{\int_{L_2}^{L_{D_2}} dz \int_{L_2}^{L_{D_2}} dz' A_o(z)A_o(z')\right\} \\
&= M_{22} + 2M_{2d} + M_{dd2} \qquad \text{(B.5)}
\end{aligned}$$

where the M_{ii} $(i = 1, 2)$ factors have been evaluated elsewhere [5] and are given by expressions (18–21) of the main text.

As far as the integrals M_{id} and M_{ddi} $(i = 1, 2)$ is concerned, we have:

$$\begin{aligned}
M_{id} &= \int_0^{L_i} dz E\left\{A_o(z)a(R_{\text{ave}})_i^b (L_{D_i} - L_i)\right\} \\
&= \frac{a^2}{\tan\varphi_i} \int_0^{L_i} dz E\left\{R^b(z)(R_{\text{ave}})_i^b \log\left(\frac{(R_{\text{ave}})_i}{10}\right)\right\} \\
&= \frac{a^2 c_i^b \log e}{\tan\varphi_i} \int_0^{L_i} dz \int_0^{\infty} dr(z) \int_{10}^{\infty} dr_{k_i} \left[r(z)^b r_{K_i}^{bd_i} \ln\left(\frac{c_i r_{K_i}^{d_i}}{10}\right) p(r(z), r_{K_i})\right]
\end{aligned} \qquad \text{(B.6)}$$

after considering again the assumptions presented in Section 2.1 and $p(r(z), r_{K_i})$ is the joint two-dimensional lognormal distribution for the

point rainrates $r(z)$ and r_{K_i}. Using now the transformations

$$\left.\begin{aligned} u_{x_i} &= \frac{\ln(r_{K_i}) - \ln R_m}{S_r} \\ u_y &= \frac{\ln(r(z)) - \ln R_m}{S_r} \end{aligned}\right\} \tag{B.7}$$

and the Bayes theorem [8] for the joint density function $f_{U_{X_i}U_y}(u_{x_i}, u_y)$ and after a tedious but straightforward algebra we have :

$$\begin{aligned} M_{id} = &\frac{a^2 \log e c_i^b R_m^{b(d_i+1)}}{\tan \varphi_i} \exp\left(\frac{b^2 S_r^2}{2}\right) \\ &\cdot \int_0^{L_i} dz \exp\left(\frac{-b^2 S_r^2 \rho_{n_i}^2(z)}{2}\right) \cdot S_i(z) \end{aligned} \tag{B.8}$$

where

$$S_i(z) = \ln\left(\frac{c_i R_m^{d_i}}{10}\right) T_i^{(1)}(z) + d_i S_r T_i^{(2)}(z) \tag{B.9}$$

and

$$\left.\begin{aligned} T_i^{(1)}(z) &= \int_{u_o}^{\infty} \exp\left[(d_i + \rho_{n_i}(z)) b u_{x_i} S_r\right] f_{U_{X_i}}(u_{x_i}) du_{x_i} \\ T_i^{(2)}(z) &= \int_{u_o}^{\infty} u_{x_i} \exp\left[(d_i + \rho_{n_i}(z)) b u_{x_i} S_r\right] f_{U_{X_i}}(u_{x_i}) du_{x_i} \end{aligned}\right\} \tag{B.10}$$

In the above expressions, $f_{U_{X_i}}(u_{x_i})$ is the normal density function [8] and $\rho_{n_i}(z)$ is the logarithmic correlation coefficient between the specific attenuations A_o and $aR_{K_i}^b$ given by:

$$\rho_{n_i}(z) = \frac{1}{b^2 S_r^2} \ln\left[1 + \rho_{o_i}(z)(e^{b^2 S_r^2} - 1)\right] \tag{B.11}$$

$$\rho_{o_i}(z) = \frac{G}{\sqrt{G^2 + (L_i - z)^2}} \tag{B.12}$$

adopting the convective raincell model, as suggested by Lin [7], to describe the spatial rainfall inhomogeneity. Following the definition of the error functions [10], the calculation of the integral (B.8) is direct

and leads to the final expressions for M_{id}:

$$M_{id} = \frac{a^2 c_i^b \log e}{2\tan\varphi_i} R_m^{b(d_i+1)} \exp\left(\frac{b^2 S_r^2 (1+d_i^2)}{2}\right) \int_0^{L_i} dz \exp[\rho_{n_i}(z) b^2 d_i S_r^2]$$
$$\cdot \left\{ \left[\ln\left(\frac{c_i R_m^{d_i}}{10}\right) + d_i^2 b S_r^2 \right] \mathrm{erfc}(a_i(z)) + b d_i S_r^2 \rho_{n_i}(z) \mathrm{erfc}(a_i(z)) \right.$$
$$\left. + \sqrt{\frac{2}{\pi}} d_i S_r e^{-a_i^2(z)} \right\} \qquad (i = 1, 2) \tag{B.13}$$

where

$$a_i(z) = \frac{u_o - b S_r (d_i + \rho_{n_i}(z))}{\sqrt{2}} \tag{B.14}$$

Finally for the M_{ddi} we have :

$$\begin{aligned} M_{ddi} &= E\left\{ \int_{L_i}^{L_{D_i}} dz \int_{L_i}^{L_{D_i}} dz' A_o(z) A_o(z') \right\} \\ &= \frac{a^2}{\tan^2\varphi_i} E\left\{ c_i^{2b} r_{K_i}^{2bd_i} \log^2\left(\frac{c_i r_{K_i}^{d_i}}{10}\right) \right\} \\ &= \frac{a^2 \log^2 e c_i^{2b}}{\tan^2\varphi_i} \int_{10}^{\infty} r_{K_i}^{2bd_i} \ln^2\left(\frac{c_i r_{K_i}^{d_i}}{10}\right) p(r_{K_i}) dr_{K_i} \end{aligned} \tag{B.15}$$

after considering again the assumption of Section 2.1. The calculation of the integral is quite trivial and gives the following expression:

$$M_{ddi} = \frac{a^2 c_i^{2b} R_m^{2bd_i}}{2\tan^2\varphi_i} \log^2 e \exp(2b^2 d_i^2 S_r^2) \left\{ \left[\left[\ell n\left(\frac{c_i R_m^{d_i}}{10}\right) + 2 b d_i^2 S_r^2 \right]^2 \right.\right.$$
$$\left. + d_i^2 S_r^2 \right] \mathrm{erfc}(u'_{oi}) + \frac{2}{\sqrt{\pi}} e^{-u'^2_{oi}} d_i S_r \left[\sqrt{2} \left(\ell n\left(\frac{c_i R_m^{d_i}}{10}\right) \right.\right.$$
$$\left.\left. + 2 b d_i^2 S_r^2 \right) + d_i S_r u'_{oi} \right] \Bigg\} \qquad (i = 1, 2) \tag{B.16}$$

where

$$u'_{oi} = \frac{u_o - 2 b d_i S_r}{\sqrt{2}} \tag{B.17}$$

APPENDIX C. EVALUATION OF THE PARAMETER ρ_{n12}

Using expressions (22) and (23) of the main text, the evaluation of ρ_{n12} leads to the calculation of the $E\{A'_C A'_I\}$ given by (see also Fig. 1):

$$\begin{aligned} E\{A'_C A'_I\} = & \int_0^{L_1} dz_1 \int_0^{L_2} dz_2 E\{A_o(z_1)A_o(z_2)\} \\ & + \int_0^{L_1} dz_1 E\left\{\int_{L_2}^{L_{D_2}} dz_2 A_o(z_1)A_o(z_2)\right\} \\ & + \int_0^{L_2} dz_2 E\left\{\int_{L_1}^{L_{D_1}} dz_2 A_o(z_1)A_o(z_2)\right\} \\ & + E\left\{\int_{L_1}^{L_{D_1}} dz_1 \int_{L_2}^{L_{D_2}} dz_2 A_o(z_1)A_o(z_2)\right\} \\ = & N_{12} + N_{1d} + N_{2d} + N_{dd} \end{aligned} \tag{C.1}$$

where the factor N_{12} has been evaluated elsewhere [3]. The calculation of N_{1d} and N_{2d} follows similar steps as those described for the evaluation of M_{id} and consequently the final results are only given:

$$\begin{aligned} N_{1d} = & \frac{a^2 c_2^b R_m^{b(d_2+1)} \log e}{2\tan\varphi_2} \exp\left(b^2 S_r^2 \left(\frac{1+d_2^2}{2}\right)\right) \\ & \int_0^{L_1} dz \exp(b^2 S_r^2 d_2 \rho_n(L_2, z, \Delta\psi)) \Bigg\{ \Bigg[\ln\left(\frac{c_2 R_m^{d_2}}{10}\right) \\ & + b d_2^2 S_r^2 + b d_2 S_r^2 \rho_n(L_2, z\Delta\psi) \Bigg] \operatorname{erfc}(a_2(z)) \\ & + \sqrt{\frac{2}{\pi}} d_2 S_r \exp(-a_2^2(z)) \Bigg\} \end{aligned} \tag{C.2}$$

where

$$\rho_n(L_2, z, \Delta\psi) = \frac{1}{b^2 S_r^2} \ln[1 + \rho_o(L_2, z, \Delta\psi)(\exp(b^2 S_r^2) - 1)] \tag{C.3}$$

$$\rho_o(L_2, z, \Delta\psi) = \frac{G}{\sqrt{G^2 + L_2^2 + z^2 - 2L_2 z\cos(\Delta\psi)}} \tag{C.4}$$

and

$$a_2(z) = \frac{u_o - (d_2 + \rho_n(L_2, z, \Delta\psi)) b S_r}{\sqrt{2}} \tag{C.5}$$

The expression for N_{2d} is the same as above but with the subscript 2 substituted by 1.

Finally for the N_{dd} we have :

$$\begin{aligned}
N_{dd} &= E\left\{\int_{L_1}^{L_{D_1}} dz_1 \int_{L_2}^{L_{D_2}} dz_2 A_o(z_1) A_o(z_2)\right\} \\
&= \frac{a^2}{\tan\varphi_1 \cdot \tan\varphi_2} E\left\{(R_{\text{ave}})_1^b (R_{\text{ave}})_2^b \log\left(\frac{(R_{\text{ave}})_1}{10}\right) \log\left(\frac{(R_{\text{ave}})_2}{10}\right)\right\} \\
&= \frac{a^2 c^{2b}}{\tan\varphi_1 \cdot \tan\varphi_2} \int_{10}^{\infty} dr_1 \int_{10}^{\infty} dr_2 r_1^{db} r_2^{db} \log\left(\frac{cr_1^d}{10}\right) \log\left(\frac{cr_2^d}{10}\right) p(r_1, r_2) \\
&= \frac{a^2 \log^2 e c^{2b} R_m^{2bd}}{\tan\varphi_1 \cdot \tan\varphi_2} \int_{u_o}^{\infty} \int_{u_o}^{\infty} du_1 du_2 e^{bdS_r u_1} \left[\ln\left(\frac{cR_m^d}{10}\right) + u_1 dS_r\right] \\
&\quad \cdot e^{bdS_r u_2} \left[\ln\left(\frac{cR_m^d}{10}\right) + u_2 dS_r\right] f_{U_1U_2}(u_1, u_2)
\end{aligned} \tag{C.6}$$

In the last expression we have used the following transformation:

$$\left.\begin{aligned} u_1 &= \frac{\ln r_1 - \ln R_m}{S_r} \\ u_2 &= \frac{\ln r_2 - \ln R_m}{S_r} \end{aligned}\right\} \tag{C.7}$$

and $f_{U_1U_2}(u_1, u_2)$ is the joint two-dimensional normal function. It should also be noted here that the approximations $c_1 \cong c_2 \cong c$, $d_1 \cong d_2 \cong d$ have been used in (C.6) in order to avoid very complicated expressions by assuming that the elevation angles φ_1 and φ_2 are not very different. By using the Bayes theorem and after a straightforward but tedious algebra we get:

$$\begin{aligned}
N_{dd} = &\frac{a^2 \log^2 e c^{2b}}{2 \tan\varphi_1 \tan\varphi_2} R_m^{2bd} \exp[b^2 d^2 S_r^2 (1 + \rho_n(L_1, L_2, \Delta\psi))] \\
&\cdot \left\{\pi_1[\text{erfc}(S_o) - K] + \pi_2 e^{-S_o^2} \text{erfc}\left(S_o \sqrt{\frac{1 - \rho_n(L_1, L_2, \Delta\psi)}{1 + \rho_n(L_1, L_2, \Delta\psi)}}\right)\right. \\
&\left. + \pi_3 e^{-2S_o^2/(1+\rho_n(L_1, L_2, \Delta\psi))}\right\}
\end{aligned} \tag{C.8}$$

where

$$\pi_1 = \left[\ln\left(\frac{cR_m^d}{10}\right) + (1+\rho_n(L_1,L_2,\Delta\psi)bd^2S_r^2\right]^2 + d^2S_r^2\rho_n(L_1,L_2,\Delta\psi) \tag{C.9}$$

$$\pi_2 = \frac{2}{\sqrt{\pi}}d^2S_r^2\rho_n(L_1,L_2,\Delta\psi)S_o + \left[\ln\left(\frac{cR_m^d}{10}\right) + d^2S_r^2b\,(1+\rho_n(L_1,L_2,\Delta\psi))\right]dS_r + \sqrt{\frac{2}{\pi}}(1+\rho_n(L_1,L_2,\Delta\psi)) \tag{C.10}$$

$$\pi_3 = \frac{1}{\pi}d^2S_r^2\sqrt{1-\rho_n^2(L_1,L_2,\Delta\psi)} \tag{C.11}$$

and

$$S_o = \frac{u_o - (1+\rho_n(L_1,L_2,\Delta\psi))bdS_r}{\sqrt{2}} \tag{C.12}$$

$$K = \frac{1}{\pi}\begin{cases} \displaystyle\int_{-\tan^{-1}(C_3)}^{\pi/2} e^{-S_o^2/\cos^2\varphi}d\varphi \\ \quad \displaystyle -\int_{-\tan^{-1}(C_3)}^{\tan^{-1}(C_1)} e^{-C_2^2/(C_1\cos\varphi-\sin\varphi)^2}d\varphi & \text{for } S_o > 0 \\ \displaystyle\int_{\tan^{-1}(C_1)}^{\pi-\tan^{-1}(C_3)} e^{-C_2^2/(C_1\cos\varphi-\sin\varphi)^2}d\varphi \\ \quad \displaystyle -\int_{\pi/2}^{\pi-\tan^{-1}(C_3)} e^{-S_o^2/\cos^2\varphi}d\varphi & \text{for } S_o < 0 \end{cases} \tag{C.13}$$

$$C_1 = \frac{\rho_n(L_1,L_2,\Delta\psi)}{\sqrt{1-\rho_n^2(L_1,L_2,\Delta\psi)}} \tag{C.14}$$

$$C_2 = \frac{S_o}{\sqrt{1-\rho_n^2(L_1,L_2,\Delta\psi)}} \tag{C.15}$$

$$C_3 = \sqrt{\frac{1-\rho_n(L_1,L_2,\Delta\psi)}{1+\rho_n(L_1,L_2,\Delta\psi)}} \tag{C.16}$$

In the above expressions, the logarithmic correlation coefficient $\rho_n(L_1, L_2, \Delta\psi)$ between ar_1^b and ar_2^b is encountered, given by:

$$\rho_n(L_1,L_2,\Delta\psi) = \frac{1}{b^2S_r^2}\ln(1+\rho(L_1,L_2,\Delta\psi)(\exp(b^2S_r^2)-1)) \tag{C.17}$$

$$\rho(L_1,L_2,\Delta\psi) = \frac{G}{\sqrt{G^2+L_1^2+L_2^2-2L_1L_2\cos(\Delta\psi)}} \tag{C.18}$$

adopting again the convective raincell model [7] to describe the spatial rainfall inhomogeneity.

REFERENCES

1. Rogers, R. R., R. L. Olsen, J. L. Strickland, and G. M. Coulson, "Statistics of differential rain attenuation on adjacent Earth-space propagation paths," *Ann. Telecommun.,* Vol. 37, No. 11–12, 445–452, 1982.
2. CCIR, "Propagation data required for evaluating interference between stations in space and those on the surface of the earth," Report 885 (MOD. I), Doc. 5 (1047-E), Inter. Telecommunication Union, Geneva, 1985.
3. Kanellopoulos, J. D., S. Ventouras, and C. N. Vazouras, "A revised model for the prediction of differential rain attenuation on adjacent Earth-space propagation paths," *Radio Science,* Vol. 25, No. 5, 853–864, 1993.
4. Crane, R. K., "Prediction of attenuation by rain," *IEEE Trans. on Commun.,* Vol. COM-28, 1717–1733, 1980.
5. Kanellopoulos, J. D., and D. Margetis, "A predictive analysis of differential attenuation on adjacent satellite paths including rain height effects," *European Transactions on Telecommunications,* Vol. 8, No. 2, 141–148, 1997.
6. Stutzman, W. L., and W. K. Dishman, "A simple model for the estimation of rain-induced attenuation along Earth-space paths at millimeters wavelengths," *Radio Science,* Vol. 17, No. 6, 1465–1476, 1982.
7. Lin, S. H., "A method for calculating rain attenuation distribution on microwave paths," *Bell Syst. Tech. J.,* Vol. 54, No. 6, 1051–1086, 1975.
8. Papoulis, A., *Probability, Random Variables and Stochastic Processes,* McGraw-Hill, New York, 1965.
9. Ha, T. T., *Digital Satellite Communications,* MacMillan, New York, 1986.
10. Abramovitz M., and I. Stegun, *Handbook of Mathematical Functions,* Dover Publications, New York, 1965.